

# Quantitative Size-Factors for Interstitial Solid Solutions

H. W. KING

*Department of Engineering and Engineering Physics, Dalhousie University, Halifax, NS, Canada*

Quantitative size-factors have been calculated from the initial slopes of volume/concentration plots for interstitial solid solutions, using data available in the literature. Solutions extending beyond 5 at. % are found to occur only in alloy systems for which the volume size-factor is less than  $30 \times 10^{-4}$ . In order of relative importance, the factors which inhibit the formation of extensive solutions are: the electronic structure, the misfit strains and the elastic coefficients. These factors are discussed for the solutions based on BCC, FCC and HCP structures.

## 1. Introduction

When quantitative size-factors based on atomic volume were presented in an earlier volume of this journal [1], no reference was made to the solutes boron, carbon, hydrogen, nitrogen and oxygen. This omission was deliberate because, in contrast to the more usual substitutional solid solutions, these elements enter into metal solid solutions by occupying the interstices between the solvent atoms. Although the concentration of interstitial solute is often quite low, these solutes can have a marked effect on the physical and mechanical properties of the solvent metal, as discussed in some detail in a recent review by Goldschmidt [2].

Since the interstitial solutes do not replace the solvent atoms at the atomic sites of the crystal structure, the solid solution will become saturated at a fixed ratio of solute:metal atoms which must always be less than 1:0. Hence, a linear extrapolation of atomic volume plots to 100% solute, does not have any physical significance for the interstitial solutions and an alternative approach must, therefore, be developed for defining quantitative size-factors.

## 2. Definition of Size-Factors for Interstitial Solid Solutions

Apart from a few solutions based on germanium, manganese or silicon, all other interstitial solid solutions are based on metals which have the BCC, FCC or HCP structure [3, 4], all of which have two different types of interstice: one bounded by six solvent atoms at the corners of an

octahedron and the other by four solvent atoms located at the corners of a tetrahedron.

In the BCC structure, the octahedral interstices are irregular, as shown in fig. 1a. The two nearest solvent atoms in this interstice lie closer to the centre of the solute atom than those which bound the regular tetrahedral interstice shown in fig. 1b. Hence, if the solvent structure is considered to remain undistorted, a larger solute atom can be accommodated in the tetrahedral interstice.

The FCC interstices are illustrated in fig. 2. Both of these are regular in shape, the octahedral hole being the larger of the two.

The shape of the interstices in the HCP structure depends on the axial ratio of the unit cell. If the axial ratio is equal to the ideal value for the close-packing of hard spheres, ( $c/a = \sqrt{8}/\sqrt{3}$  or 1.6330), these interstices become the same size and shape as those in the FCC structure, as shown in fig. 3. Since, however, the ideal axial ratio is not observed in any of the pure metals [3], the interstices in the HCP solid solutions are distorted from regular octahedra or tetrahedra. Even so, the nature of this distortion is such that in both the interstices the solute atom remains equidistant from the surrounding solvent atoms.

Crystallographic relationships for calculating the distance from the centre of an octahedral or tetrahedral interstice to the centre of the nearest solvent atom (i.e.  $S_O$  or  $S_T$ ) are summarised in table I. The maximum radius of a spherical solute atom which can enter into a particular interstice

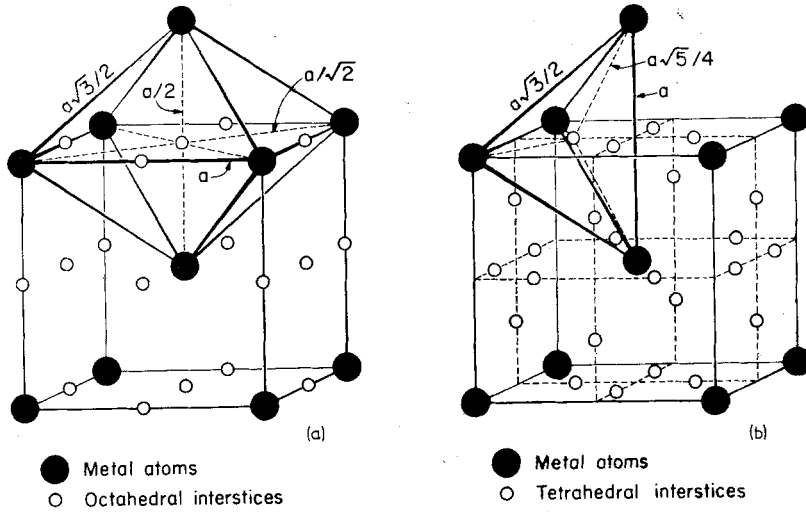


Figure 1 Interstitial holes in the BCC structure, (a) Octahedral holes at face centres and cell edges. (b) Tetrahedral holes on cell faces.

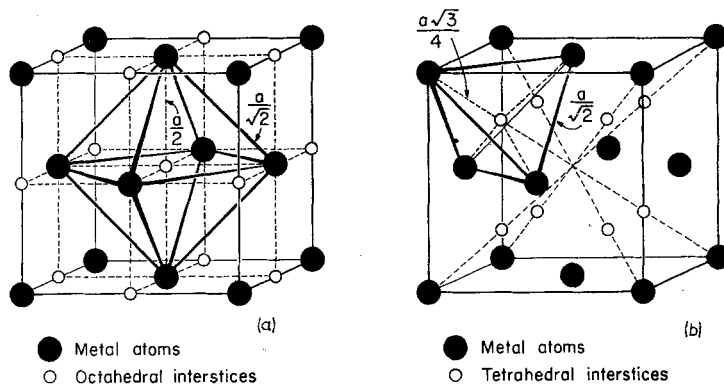


Figure 2 Interstitial holes in the FCC structure, (a) Octahedral holes at body centre and mid-points of cell edges. (b) Tetrahedral holes on body diagonals.

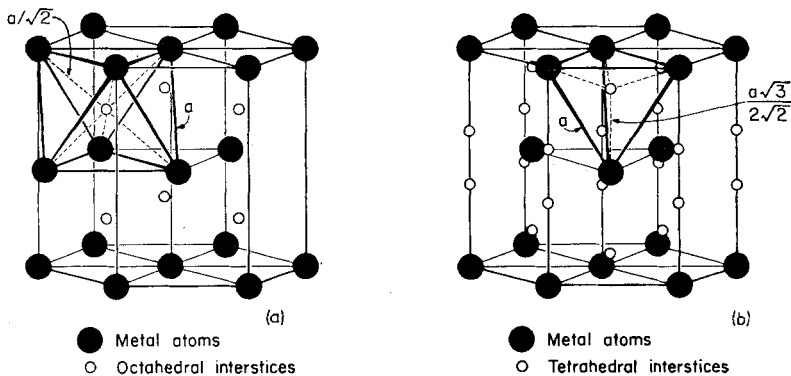


Figure 3 Interstitial holes in the HCP structure, (a) Octahedral holes within the cell  $(\frac{1}{3}, \frac{1}{3}, z_1; \frac{2}{3}, \frac{2}{3}, 1 - z_1)$ . (b) Tetrahedral holes along cell edges  $(0, 0, -z_2; 0, 0, \frac{1}{2} + z_2)$  and within the cell  $(\frac{2}{3}, \frac{1}{3}, z_2; \frac{2}{3}, \frac{1}{3}, 1 - z_2)$ . As drawn above for ideal  $c/a$ ,  $z_1 = \frac{1}{4}$ ;  $z_2 = \frac{1}{8}$ . For general values of interatomic distances and clearance holes see table I.

TABLE I Some useful relationships for interstices in metal structures

Parameter	BCC	FCC	HCP Ideal $\frac{c}{a}$	HCP $\frac{c}{a} > \frac{\sqrt{8}}{\sqrt{3}}$	HCP $\frac{c}{a} < \frac{\sqrt{8}}{\sqrt{3}}$
$R_A$	$a \cdot \frac{\sqrt{3}}{4}$ (0.433a)	$a \cdot \frac{\sqrt{2}}{4}$ (0.3536a)	$a \cdot \frac{1}{2}$ (0.5a)	$a \cdot \frac{1}{2}$ (0.5a)	$\frac{a}{2\sqrt{3}} \sqrt{1 + \frac{3}{4} \left(\frac{c}{a}\right)^2}$ ( $\sqrt{0.0833a^2 + 0.0625c^2}$ )
$S_O$	$a \cdot \frac{1}{2}$ (0.5a)	$a \cdot \frac{\sqrt{2}}{2}$ (0.707a)	$a \cdot \frac{1}{2}$ (0.5a)	$a \cdot \frac{\sqrt{2}}{2}$ (0.707a)	$\frac{a}{\sqrt{3}} \sqrt{1 + \frac{3}{16} \left(\frac{c}{a}\right)^2}$ ( $\sqrt{0.3333a^2 + 0.0625c^2}$ )
$R_A \cdot \frac{2}{\sqrt{3}}$	$R_A \cdot \frac{\sqrt{8}}{\sqrt{3}}$	$R_A \cdot \sqrt{2}$	$R_A \cdot \sqrt{2}$	$R_A \cdot \frac{2}{\sqrt{3}} \sqrt{1 + \frac{3}{16} \left(\frac{c}{a}\right)^2}$	$R_A \cdot 2 \sqrt{\frac{1 + \frac{3}{16} \left(\frac{c}{a}\right)^2}{1 + \frac{3}{4} \left(\frac{c}{a}\right)^2}}$
$R_O$	(0.067a)	(0.274a)	(0.1464a)	(0.207a)	$(S_O - R_A)$
	(0.1547 $R_A$ )	(0.633 $R_A$ )	(0.4142 $R_A$ )	(0.4142 $R_A$ )	$\left[ \sqrt{1.333 + 0.25 \left(\frac{c}{a}\right)^2} - 1 \right] R_A$
					$\left[ \sqrt{\frac{4 + 0.75 \left(\frac{c}{a}\right)^2}{1 + 0.75 \left(\frac{c}{a}\right)^2}} - 1 \right] R_A$
$S_T$	$a \cdot \frac{\sqrt{5}}{4}$ (0.559a)	$a \cdot \frac{\sqrt{3}}{4}$ (0.433a)	$a \cdot \frac{\sqrt{3}}{\sqrt{8}}$ (0.6124a)	$\frac{a}{3} \left( \frac{a}{c} + \frac{3c}{4a} \right)$ ( $0.3333 \frac{a^2}{c^2} + 0.25c$ )	$\frac{a}{3} \left( \frac{a}{c} + \frac{3c}{4a} \right)$ ( $0.333 \sqrt{\frac{a^2}{c^2} + 0.25c}$ )
	$R_A \cdot \frac{\sqrt{5}}{\sqrt{3}}$	$R_A \cdot \frac{\sqrt{3}}{\sqrt{2}}$	$R_A \cdot \frac{\sqrt{3}}{\sqrt{2}}$	$R_A \cdot \frac{2}{3} \left( \frac{a}{c} + \frac{3c}{4a} \right)$	$R_A \cdot \frac{2}{\sqrt{3}} \sqrt{\left(\frac{a}{c}\right)^2 + \frac{3}{4}}$
$R_T$	(0.126a)	(0.0794a)	(0.1124a)	$(S_T - R_A)$	$(S_T - R_A)$
	(0.211 $R_A$ )	(0.2248 $R_A$ )	(0.2248 $R_A$ )	$\left[ 0.6666 \frac{a}{c} + 0.25 \frac{c}{a} - 1 \right] R_A$	$\left[ \sqrt{1 + 1.333 \left(\frac{a}{c}\right)^2} - 1 \right] R_A$

without distorting the solvent structure can thus be obtained by taking

$$R_O = S_O - R_A \text{ or } R_T = S_T - R_A \quad (1)$$

where  $R_A$  is the atomic radius of the solvent. The latter is conveniently derived from the lattice constants of the solvent structure, assuming that the atoms are hard spheres in contact with each other, again using relationships listed in table I. It should be noted in passing, that although this definition of atomic radius is inapplicable to solute atoms, which change their size when dissolved in solvents of different valence or coordination [1, 5, 6], it is appropriate for the solvent atoms, because these remain in the same crystal structure.

For practical purposes, it is convenient to express  $R_O$  or  $R_T$  as a fraction of the solvent radius  $R_A$  and the appropriate relationships are also included in table I. The use of the ratio  $R_O/R_A$  or  $R_T/R_A$  allows the size of a particular interstice to be compared directly with the size-factor proposed by Hägg [7], namely  $R_I/R_A$ , where  $R_I$  is the radius of the interstitial atom derived from interatomic distances in its elemental form. Like the Hume-Rothery size-factor for substitutional solid solutions, the Hägg size-factor has also been used as the basis of an empirical rule based on a study of the compounds formed by the transition metals and the elements boron, carbon, hydrogen and nitrogen. Hägg observed that when the ratio  $R_I/R_A$  is less than

0.59, the intermetallic compounds formed at compositions  $A_4I$ ,  $A_2I$ ,  $AI$  and  $AI_2$  can be expressed in terms of a simple metallic structure (i.e. FCC, HCP etc.) with the metalloids occupying the interstices. Since there are no metalloid-metalloid contacts, these compounds have distinctly metallic properties, in contrast to compounds such as  $Fe_3C$  which form in systems for which  $R_I/R_A$  is greater than 0.59. The ratio  $R_I/R_A$  should not be taken as a measure of the misfit strain, however, since it takes no account of the possible change in the atomic size of the solute, an effect which is often quite significant in these solutions [6].

Since quantitative size-factors have their application in understanding the properties of the solution—not the solute—they may be defined from observed lattice parameters, with-

out involving the concept of the effective size of the solute. Thus, using the sphere-in-the-hole-model, and following Darken and Gurry [8] and Eshelby [9], the strain energy stored in a solvent matrix at a given fractional composition  $c$  is given by

$$E_s(c) = \frac{2}{3}\mu\Omega\left(\frac{1}{\Omega}\cdot\frac{\partial\Omega}{\partial c}\right)^2 f(c) \quad (2)$$

where  $\mu$  and  $\Omega$  refer to the shear modulus and the atomic volume of the solvent matrix and  $f(c)$  is linear for low values of  $c$ . A study of the available lattice parameter data for interstitial solid solutions [3] shows that the atomic volume varies linearly with atomic concentration of solute up to a limiting composition which may be referred to as  $c_l$ . The parameter  $[1/\Omega \cdot (\partial\Omega/\partial c)]$ , which appears in the strain energy equation above,

TABLE II Size-factors for interstitial solid solutions—I BCC and complex cubic structures

System	$\Omega_A$ (Å)	$R_A$ (Å)	$c_{sat}$ (at. %)	$\Omega sf$ ( $\times 10^4$ )	$lsf$ ( $\times 10^4$ )	$c_l$ (at. %)	$R_I/R_A$
<i>BCC</i>							
$C_8$ -O	113.056	2.6375	?	(+ ve)	(+ ve)	—	0.227
$\alpha$ Fe-B	11.774	1.2411	< 0.02	(- ve)	(- ve)	?	0.733
-C			0.11	(78.1)	(21.2)	0.1	0.620
-H			1.5	(9.7)	(3.2)	1.5	0.371
-N			0.4	(70.5)	(19.5)	0.4	0.572
-O			< 0.03	(- ve)	(- ve)	?	0.483
Mo-C	15.578	1.3625	0.15	(62.9)	(17.7)	0.1	0.565
Nb-C	17.972	1.5290	8	(24.1)	(7.5)	0.3	0.539
-H*			~ 50	20.3	6.4	10	0.322
-N			11.5	(22.2)	(6.9)	0.3	0.497
-O			9	25.5	7.9	4.8	0.420
Ta-B	18.016	1.4302	2	(+ ve)	(+ ve)	?	0.636
-C			5	(12.8)	(4.1)	0.1	0.538
-H			~ 50	19.1	6.0	28.5	0.322
-N			12	40.7	12.1	4.8	0.496
-O			6	43.0	12.6	3.6	0.420
V-C	13.851	1.3102	8.7	(+ ve)	(+ ve)	?	0.587
-H			~ 50	(24.9)	(7.68)	4	0.351
-O			~ 4	79.5	21.5	3.2	0.458
W-C	15.849	1.3704	0.3	(6.7)	(1.3)	0.3	0.562
<i>Complex cubic</i>							
Ge-O	22.482	1.222	60	0.2	0.1	56.9	0.490
$\alpha$ Mn-C	12.212	1.12	8.5	(37.2)	(11.1)	8.5	0.688
-H			?	(+ ve)	(+ ve)	—	0.411
-N			0.5	(34.2)	(10.31)	0.5	0.634
$\beta$ Mn-N	12.590	1.18	5	(6.1)	(2.0)	5	0.602
Si-B	20.01	1.175	3.6	- 80.0	- 21.6	3.6	0.774

may therefore be derived from the initial slopes of volume/concentration plots and the atomic volume  $\Omega_A$  of the solvent, to give a volume size-factor for the solution, defined as

$$\Omega_{sf} = \frac{1}{\Omega_A} \left( \frac{\partial \Omega}{\partial c} \right) \quad (3)$$

A linear size-factor can be derived from  $\Omega_{sf}$  following the analysis given previously [5], i.e.

$$l_{sf} = (\Omega_{sf} + 1)^{1/3} - 1 \quad (4)$$

The size-factors defined above are formally equivalent to those derived for substitutional solutions [1] (even though they do not require a knowledge of the effective size of the solute atom) and can be used in a quantitative manner when analysing the effect of misfit strains on the physical, chemical or mechanical properties of interstitial solid solutions.

### 3. Size-Factor Determinations

Although interstitial primary solid solutions extending beyond 0.5 at. % solute have been reported for some ninety binary alloy systems [4], it is disappointing to find that the compositional dependence of the lattice parameters has been measured in only fifty of these solutions. The alloy for which data are particularly lacking are those based on the rare earths, many of which dissolve up to 50 at. % of interstitial solutes at high temperatures.

Using the data collected by Pearson [3], size-factors have been calculated according to equations 3 and 4, the results being listed according to the crystal structure of the solvent in tables II and III. For convenience of presentation, the results have been scaled by a factor  $10^4$ . In this form the numerical values in the tables can be compared directly with those given

TABLE III Size-factors for interstitial solid solutions—II FCC and HCP structures

System	$\Omega_A$ ( $\text{\AA}^3$ )	$R_A$ ( $\text{\AA}$ )	$c_{\text{sat}}$ (at. %)	$\Omega_{sf}$ ( $\times 10^4$ )	$l_{sf}$ ( $\times 10^4$ )	$c_l$ (at. %)	$R_l/R_A$
<b>FCC</b>							
Ce-B	34.371	1.8250	?	(- ve)	(- ve)	—	0.499
-C			~ 50	- 15.5	- 4.92	11.5	0.421
-H			~ 50	(1.7)	(0.6)	16.6	0.252
$\alpha$ Co-C	11.109	1.2525	4.5	(+ ve)	(+ ve)	?	0.615
-N			3.8	(84.8)	(22.7)	2.5	0.569
Pd-H	14.728	1.3759	~ 5	4.2	1.4	5	0.334
Pt-H	15.104	1.3874	~ 0.02	(+ ve)	(+ ve)	?	0.332
Th-B	32.918	1.7989	?	(- ve)	(- ve)	—	0.506
-C*			15	50.0	14.7	2.5	0.428
<b>HCP</b>							
$\alpha$ Hf-B	22.317	1.5636	0.5	(+ ve)	(+ ve)	?	0.582
-N			29	10.5	3.4	29	0.454
-O			21.5	6.2	2.0	21.5	0.384
†Mg-H	22.524	1.5826	?	(+ ve)	(+ ve)	—	0.288
Re-C	14.705	1.3699	11.7	(22.5)	(7.0)	11.7	0.562
Tc-B	14.297	1.3544	~ 8.5	(+ ve)	(+ ve)	?	0.672
-C			7.7	(+ ve)	(+ ve)	?	0.569
$\alpha$ Ti-B*	17.638	1.4469	~ 33	10.8	3.5	18	0.629
-C			2	48.2	14.0	1.6	0.532
-H			8	(+ ve)	(+ ve)	?	0.318
-N			20	22.5	7.0	17	0.491
-O*			~ 33	14.8	4.7	25	0.415
$\alpha$ Zr-B	23.356	1.5908	2	(+ ve)	(+ ve)	?	0.573
-H			6	(+ ve)	(+ ve)	?	0.289
-O*			~ 33	9.07	2.9	20	0.378

†This alloy also contains 10% Al, 0.2% Mn and 1.7% Zn.

previously for the substitutional solid solutions [1]. The values listed within brackets refer to size-factors derived from the lattice parameters of supposedly saturated solid solutions, the compositions of which were not checked by chemical analysis [3], but estimated from phase diagram information [4]. These results are included to indicate the general trend of the volume changes in these alloy systems and thus should not be used in a quantitative manner to derive a volume for a particular alloy concentration.

The concentration limit to which appropriate size-factors may be applied for calculating lattice strains is indicated by  $c_l$  in column 7 of tables II and III. These concentrations are equivalent to those referred to as  $c_{\max}$  for substitutional solutions [1], but the nomenclature has been changed to avoid possible confusion with  $c_{\text{sat}}$  — the concentration of the saturated solid solution, which may not necessarily refer to room temperature. In most of the systems studied,  $c_l$  is considerably lower than  $c_{\text{sat}}$ . This can occur either because alloys have not been examined across the entire solid solution, or because the linear relationship between volume and composition only holds at low concentrations, so that the volume plots tend to flatten out beyond  $c_l$ . The latter situation occurs in the systems marked with an asterisk, i.e. Nb-H, Th-C, Ti-B, Ti-O and Zr-O and does not appear to be related to a particular type of solvent structure. For example, although it occurs in BCC Nb-H it is absent in Ta-H, and again while it occurs in HCP Ti-O and Zr-O, it is absent in Hf-O. There also appears to be no direct relationship between the occurrence of this effect and the magnitude of  $\Omega_{sf}$ .

Radius ratios,  $R_I/R_A$ , have also been calculated for the solutions under investigation and are included in column 8 of tables I and II.

## 4. Discussion

### 4.1. Negative Size-Factors

A study of the size-factors listed in table II and III shows that a number of them are negative, indicating that a decrease in volume occurs on alloying. This was unexpected, since one would expect that in general the solute atoms would be too large to fit into the available interstices of the solvent structure and hence any lattice distortion would take the form of an expansion rather than a contraction.

The negative size-factors for  $\alpha\text{Fe-O}$  and Th-B should not be taken too seriously, perhaps,

because in both cases they are based on single alloys of unknown chemical composition, whose lattice parameters in any event lie within the scatter of the experimental values for the pure solvents [3]. The solution of boron in silicon, on the other hand, is considered to be substitutional in nature and the same conclusion has been drawn for  $\alpha\text{Fe-B}$ , on the basis of internal friction measurements [2-4].

This leaves Ce-C as the only unquestionable instance of a negative lattice distortion, in an interstitial solution which extends up to 11.5 at. %. Since cerium has the largest atomic volume of the FCC solvents in table III, the possibility exists that the carbon atoms enter the solution without expanding the lattice. The minimum atomic volumes of solvents at which the five interstitial solutes can enter the various interstices without distorting the solvent structure are listed in table IV. These values are more

TABLE IV Atomic volumes ( $\text{\AA}^3$ ) of solvents at which  $R_O$  or  $R_T = R_I$

Solute	$R_I$ ( $\text{\AA}$ )	BCC		FCC and HCP (ideal)		
		$\Omega_O$	$\dagger\Omega_O'$	$\Omega_T$	$\Omega_O$	$\Omega_T$
B	0.91	1250	18.3	188	63.1	375
C	0.77	758	11.1	114	38.3	227
N	0.71	536	8.7	89.2	29.9	178
O	0.60	360	5.2	53.9	18.1	108
H	0.46	162	2.4	24.3	8.1	48.5

$\dagger\Omega_O'$  = Volume at which  $R_I$  equals the larger clearance distance in the irregular octahedral hole of the BCC structure (see fig. 1).

convenient than the limiting values of the radius ratio  $R_I/R_A$ , since the atomic volumes of the elements are listed in standard tables. It is readily apparent from table IV that cerium, with an atomic volume of  $34.37 \text{\AA}^3$  lies just below the limiting value for the solution of carbon in the octahedral interstices of the FCC structure. The solution would thus be expected to show a very small increase in atomic volume with carbon concentration. It is also known, however, that cerium can exist in two FCC forms, one of which has a 16% smaller atomic volume, which is associated with the transfer of electrons from the outer 6s band to the inner 4f band [3, 4]. This observation is a particular manifestation of the general contraction which occurs as the 4f band is progressively filled across the lanthanide series of elements [10]. Hence, if the valence electrons

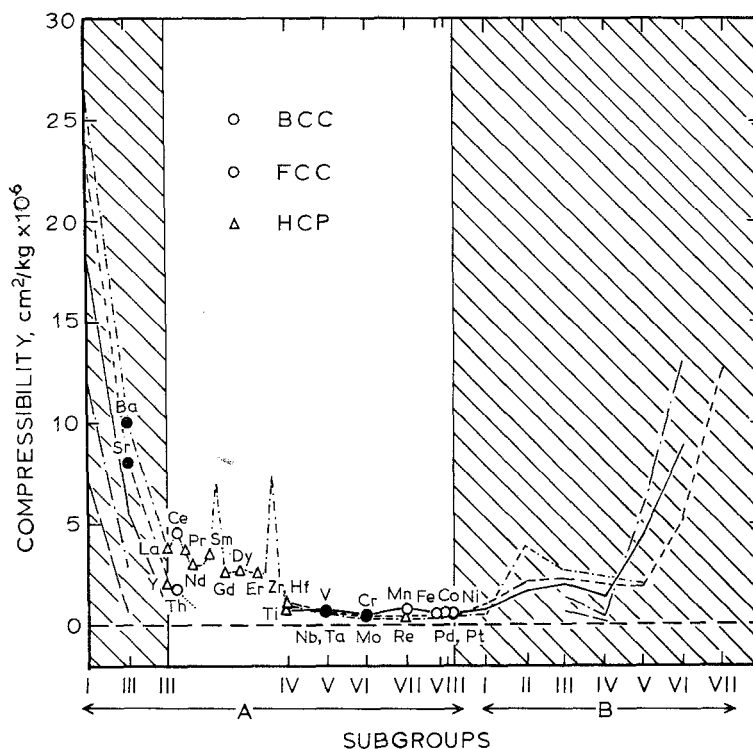


Figure 4 Solvents which form extensive interstitial solutions indicated on plots of compressibility versus sub-group number, for different periods of the periodic table.

of carbon enter the 4f band of cerium, a similar volume contraction would be expected across the Ce-C solid solution, which would account for the negative size-factor in table III.

#### 4.2. The Effect of Size-Factors on Solubility Limits

The significance of the electronic structure and the elastic properties of the solvent on the formation of extensive interstitial solid solutions is illustrated in fig. 4, where the solvents which form solutions beyond 1 at. % are indicated on plots of compressibility versus sub-group number for different periods of the periodic table [10]. It is readily apparent that, in spite of their relatively high compressibilities, none of the elements from group IA or from any of the B-sub-groups form extensive solid solutions, while the elements Ba and Sr from group IIA only form extensive solutions with hydrogen. This pattern of behaviour can be attributed to the general tendency of these elements to form ionic or covalent compounds when alloyed with the metalloids [3, 4]. The rare earths and the

transition metals, on the other hand, can retain their essentially metallic character by absorbing the valence electrons from the solutes into their unfilled f- or d- bands [2], as mentioned above for Ce-C. Granted that the electronic factors limit the formation of extensive interstitial solid solutions to the latter series of elements, it is important to notice, by comparing the data in tables II and III, that the rare earths and the group IVA metals Ti, Zr and Hf show a greater tendency to form extensive solid solutions than the remaining transition metals, which have significantly lower compressibilities. Hence, after the basic electronic condition has been satisfied, the solubility limit is governed by the elastic properties of the solvent matrix.

When the size-factors in tables II and III are compared with the solubility limits  $c_1$ , beyond which the volume changes are no longer linear with composition, it is found that values of  $c_1$  greater than 5 at. % only occur when  $\Omega sf$  is less than 30% ( $Isf < 10\%$ ), regardless of the structure of the solvent. This limit on the size-factor is precisely the same as that observed

previously for the substitutional solid solutions [1, 10] and lies well within the theoretical limit derived from calculations based on the sphere-in-the-hole model [5, 8, 9]. In this connection, it is also of interest to note that the size-factors for interstitial solutions are of much the same order of magnitude as those for substitutional solutions, which again confirms that the upper limit of the lattice distortion is governed by the elastic properties of the solvent matrix.

When the size-factors are compared with  $c_{\text{sat}}$ , the solute concentration at saturation, however, there is no definite cut-off when the volume size-factor rises above 30%. In the system Th-C, for example,  $\Omega_{sf} = 50\%$ , yet  $c_{\text{sat}}$  extends to 15 at. %. This discrepancy occurs because the volume/concentration plot is not linear across the entire solid solution. Hence, the  $\Omega_{sf}$  value of 50% is indicative of a high initial rate of lattice distortion at concentrations up to  $c_1 (= 2.5 \text{ at. \% C})$ , beyond which the rate of distortion falls to a lower, steadier value. Using the latter slope, the  $\Omega_{sf}$  for this alloy system for the range of composition from 10 to 15 at. % C is found to be 21.4, i.e. well within the 30% limit referred to above. A similar fall in size-factor beyond  $c_1$  also occurs in the systems Nb-H, Ti-B, Ti-O and Zr-O.

A further reason for an apparent discrepancy between  $c_{\text{sat}}$  and the 30% limit of the volume size-factor, is that many of the solubility limits refer to high temperatures, at which a higher degree of lattice distortion can be tolerated due to softening of the elastic constants of the solvent. In Ta-N and Ta-O, for example,  $c_{\text{sat}}$  extends beyond 5 at. %, yet the  $\Omega_{sf}$  values are greater than 40%. The  $c_{\text{sat}}$  values quoted in table II for these alloy systems refer to temperatures above 1600°C, however, but the equivalent room temperature values are less than 1 at. % [4] and thus conform to the empirical rule established above.

### 4.3. The Influence of Solvent Structure

The limited number of size-factor values presented in tables II and III makes it difficult to assess whether or not the relative magnitude of  $\Omega_{sf}$  is related to the crystal structure of the solvent. The complex cubic solutions, for example, show the same spread in  $\Omega_{sf}$  values as the FCC and BCC solutions and hence the only indication of any kind of pattern is that the highest value of  $\Omega_{sf}$  for the HCP solutions ( $\sim 50 \times 10^{-4}$ ) is significantly lower than the maximum values ( $\sim 80 \times 10^{-4}$ ) for the cubic solutions.

#### 4.3.1. BCC solutions

The largest number of  $\Omega_{sf}$  values for a given solvent structure occurs for the BCC solutions. This is somewhat surprising since (as may be seen from tables II and IV) none of the BCC solvents apart from Ce has a large enough atomic volume to accommodate even hydrogen without some lattice distortion. Nevertheless, solutions extending up to 50 at. % do occur for BCC solvents, but only when hydrogen is the solute. Solutions greater than 5 at. % occur when carbon, nitrogen or oxygen are dissolved in the VA solvents V, Nb and Ta, but only at high temperatures. Hence the  $c_1$  limits for these solutions, which are based on room temperature lattice parameter data, do not exceed 5 at. %. Higher values occur for Nb-H and Ta-H, for which the atomic volumes of  $\sim 18 \text{ \AA}^3$  lie just below the  $\Omega_T$  for hydrogen (table IV).

It is interesting to note that BCC  $\alpha$ -Fe, with an atomic volume of  $11.774 \text{ \AA}^3$  lies well below any of the  $\Omega_T$  limits given for the solutes in table IV, yet this phase dissolves a measurable concentration of all of the interstitial solutes. Evidence from internal friction, etc [2], indicates that while boron enters  $\alpha$ -Fe substitutionally the remaining solutes occupy the smaller irregular octahedral interstices (fig. 1), by displacing only the two nearest solvent atoms. Providing the concentration is low and the sites are occupied at random, the net effect of these displacements is an overall increase in atomic volume. If the sites are occupied by a limited number of solute atoms but in an ordered fashion, as in  $\alpha'$ -martensite [2], the structure distorts uniformly to BCT. This proposal is confirmed by the data in table IV, which show that the various values of  $\Omega_{O'}$  (except for boron) all lie below the atomic volume of  $\alpha$ -Fe and hence the solutes can enter the octahedral interstices without displacing, or even making contact with, the four second nearest solvent atoms. The limiting radius ratio for this situation is given by  $R_{O'}/R_A = 0.633$ , as indicated in table I.

When the solubility limits,  $c_{\text{sat}}$ , of the BCC solutions are plotted as a function of the radius ratio,  $R_I/R_A$ , as shown in fig. 5, it is found that all the extensive solutions apart from a few containing boron, occur in systems for which  $R_I/R_A$  is less than 0.633. It is interesting to note that this radius ratio is close to the limiting value of 0.59 proposed by Hägg for intermediate compounds with simple metallic structures, even though he was unable to find a truly BCC



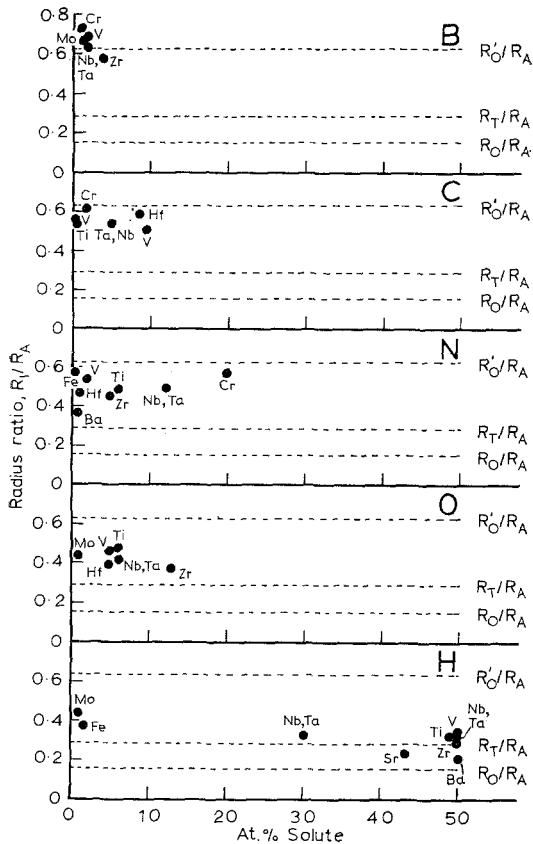


Figure 5 Limits of saturated solid solution,  $c_{\text{sat}}$ , plotted against the radius ratio  $R_I/R_A$  for BCC interstitial solutions.

compound which conformed to his rule [7]. A closer study of fig. 4 indicates that hydrogen, and to a lesser extent oxygen, can be accommodated in the regular tetrahedral interstices provided the solvent matrix is reasonably soft elastically. The occupancy of the irregular octahedral sites becomes more pressing in solutions containing nitrogen and carbon, however, particularly for the small atomic volume solvents from the first long period of the periodic table, most of which have  $R_I/R_A$  values between 0.5 and 0.6.

#### 4.3.2. FCC and HCP solutions

When the atomic volumes of the FCC solvents in table III are compared with the  $\Omega_0$  limits in table IV it is not surprising to find that extensive solutions only occur for carbon and hydrogen dissolved in cerium and for carbon in thorium. The HCP solvents, on the other hand, form extensive solutions with both carbon and nitrogen, even though their atomic volumes lie

considerably below the  $\Omega_0$  limits for these solutes in table IV. Since the latter limits are only applicable to ideally close-packed HCP solvents, it follows that the axial ratio of the solvent must play an important role, along with the atomic volume, in determining the solubility limits of these interstitial solutions.

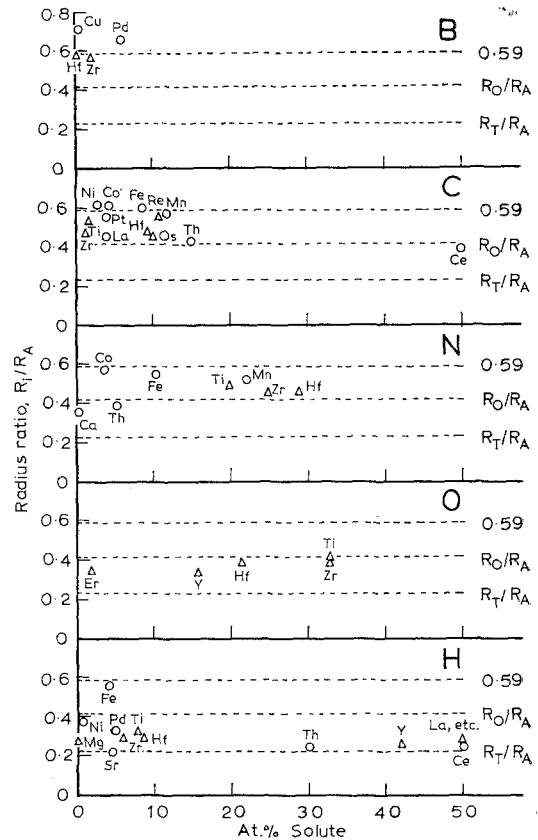


Figure 6 Limits of saturated solid solution,  $c_{\text{sat}}$ , plotted against the radius ratio  $R_I/R_A$  for FCC and HCP interstitial solutions.

To examine the difference between the FCC and HCP solutions in more detail, values of  $c_{\text{sat}}$ , taken from the literature [4], are plotted against the radius ratio,  $R_I/R_A$ , in fig. 6. The radius ratios for the HCP solutions are calculated using the expressions given in table I and thus take account of the particular  $c/a$  of the solvent metal. It is immediately apparent from this plot that Hägg's radius ratio limit of 0.59 is convincingly demonstrated to be applicable to both the FCC and HCP solutions. It is also noticeable that, with the exception of Cu-B (which is probably a substitutional solution),

there is a distinct lack of interstitial solutions based on the IB FCC metals, Cu, Ag and Au, even though their atomic volumes (15 to 18 Å<sup>3</sup>) lie within the  $\Omega_0$  limit for hydrogen, and close to that of oxygen. This absence is all the more surprising in view of the tendency of these metals to form extensive substitutional solutions, often with considerable lattice distortion [3], with the other B-sub-group elements as solutes [4]. As mentioned above, the general lack of interstitial solutions based on the B-sub-group metals is attributed to the absence of an incomplete inner electronic band in these metals.

The radius ratios for the hydrogen solutions in fig. 6 are low enough to permit the solute atoms to be accommodated in the smaller tetrahedral interstices. This is confirmed by the structure of the hydrides of the transition metals and the rare earths, most of which have the C<sub>1</sub>CaF<sub>2</sub> structure, in which the metal atoms lie at FCC positions and the solute atoms occupy the tetrahedral interstices [2, 3]. The equivalent oxide, nitride and carbide compounds of these elements have the B<sub>1</sub>NaCl structure, or the hexagonal W<sub>2</sub>C structure, in both of which the solute atoms occupy the octahedral interstices [2, 3, 7]. The radius ratio values of the solutions in fig. 6 indicate that oxygen, nitrogen and carbon also occupy the octahedral interstices when entering the FCC or HCP solid solutions.

It is also apparent from fig. 6, that only HCP solvents form extensive solutions with oxygen, but this may reflect a lack of study of the FCC solutions, rather than a general trend. Although FCC solutions occur with nitrogen as solute, they have significantly lower  $c_{\text{sat}}$  values than the HCP solutions, even though in the case of Ca and Th they have more favourable radius ratios. Apart from Ce and Th, all solutions containing carbon involve a considerable distortion of the octahedral interstices. There appears to be no clear distinction between the  $c_{\text{sat}}$  limits of these FCC and HCP solutions, but the situation is confused because the FCC solutions can exist at higher temperatures than the HCP solutions, because of the HCP  $\rightleftharpoons$  BCC allotropic change which occurs in Ti, Zr and Hf. There is a general trend, nevertheless, that the HCP solvents tend to form more extensive solutions than FCC solvents of equivalent atomic volume.

The difference between the FCC and HCP structure arises because the co-ordination of the latter changes from 12 to 6,6 when the axial ratio deviates from the ideal value for close-

packing. A study of the geometry of the HCP interstices shows that, no matter whether the deviation in axial ratio increases the separation of the atoms in the basal planes or the pyramidal planes, the radius of the clearance hole for both the octahedral and tetrahedral interstices (i.e.  $R_O$  or  $R_T$ ) is thereby *increased*. This is demonstrated in table V, in which the values of  $R_O/R_A$  and  $R_T/R_A$  have been calculated for some typical HCP metals. It is of interest to note, in passing, that although the interstices in Zn and Cd are considerably enlarged due to their high axial ratios, neither of these B-sub-group metals forms an extensive interstitial solution. It is also evident from table V that the solvents Ti, Zr and Hf, which have axial ratios well below the ideal value, thus have significantly larger clearance holes than an FCC solvent of the same atomic volume.

On the basis of misfit strains alone, it is to be expected that the axial ratio should deviate progressively from the ideal value across an HCP solid solution. In practice, however, this trend is only observed in solutions based on the VIIA solvents Tc and Re. The extensive solutions based on the IVA solvents Ti, Zr and Hf show just the opposite trend, i.e. a change in  $c/a$  towards the ideal value. The axial ratio of an HCP metal is, however, governed primarily by the electronic band structure. Hence on adding a solute, the influence on the band structure must be considered, along with the effect of misfit strains, in altering the overall energy of the alloy. If the band structure contribution to the energy demands a change of axial ratio towards the ideal value on alloying with a particular solute, this axial ratio change can only occur if the elastic constants of the alloy are sufficiently soft to allow an overall increase in volume which more than off-sets the decrease in the size of the interstices due to the change in axial ratio. This situation appears to hold for the group IVA metals as shown by the  $c/a$  and  $R_O/R_A$  values for the saturated solid solutions listed in table V. These metals also have a relatively high compressibility, as indicated by the data plotted in fig. 4. If, on the other hand, the solvent is relatively incompressible, as in the case for Tc and Re (see fig. 4), then, if the atomic volumes are not too favourable, interstitial solutions can only occur if the misfit strains are accommodated by a progressive deviation away from the ideal axial ratio.

On the basis of the above discussion, the factor

TABLE V The effect of axial ratio on the interstices in HCP metals and alloys

Metal solvent	$c/a$	$R_O/R_A$	$R_T/R_A$	Saturated solution	$c/a$	$R_O/R_A$	$R_T/R_A$
Be	1.5684	0.432	0.242	—	—	—	—
Hf	1.5817	0.429	0.238	Hf-B	1.5886	0.436	0.244
				-N	1.6010	0.446	0.253
				-O	1.5857	0.440	0.247
Ti	1.5857	0.428	0.237	Ti-B	1.6107	0.446	0.252
				-C	1.5914	0.432	0.240
				-H	1.6062	0.434	0.242
				-N	1.6103	0.446	0.252
				-O	1.6364	0.447	0.253
Zr	1.5917	0.426	0.235	Zr-B	1.5957	0.435	0.243
				-H	1.5928	0.427	0.236
				-O	1.6001	0.434	0.242
Tc	1.6051	0.422	0.232	Tc-B	1.6028	0.426	0.235
				-C	1.5838	0.454	0.259
Re	1.6152	0.419	0.229	Re-C	1.6014	0.432	0.240
†Mg	1.6259	0.416	0.226	†Mg-H	1.6263	0.419	0.229
IDEAL	1.6330	0.414	0.225	—	—	—	—
Zn	1.8549	0.481	0.287	—	—	—	—
Cd	1.886	0.491	0.296	—	—	—	—

† This alloy also contains 10% Al, 0.2% Mn and 1.7% Zn.

Notes: (1) For solvents,  $R_O/R_A$  and  $R_T/R_A$  are calculated using the expressions given within square-brackets in table I.

(2) For solutions,  $R_O$  and  $R_T$  are derived by subtracting  $R_A$ , for the solvent, from  $S_O$  and  $S_T$  using the expressions given with the curved brackets in table I.

influencing interstitial solid solutions may be listed in an order of priority, viz.

(1) Electronic factors are primary and can eliminate complete sub-groups of possible solvents.

(2) Size-factors, as determined by volumes and (where necessary) by axial ratios, are secondary, coming into effect only when electronic conditions are satisfied. Extensive solutions only occur when  $\Omega sf$  is less than  $30 \times 10^{-4}$ .

(3) Elastic coefficients of the solvent are tertiary, only becoming operative when both electronic and size-factor conditions are satisfied. The elastic properties govern the extent of the solution rather than its essential formation or prohibition.

### Acknowledgements

The Author is grateful to Professor J. G. Ball for his helpful advice and encouragement and to Mr M. Sampson and Mr P. Ormiston, for their help with the volume calculations and literature searches.

### References

1. H. W. KING, *J. Mater. Sci.* **1** (1966) 79.
2. H. J. GOLDSCHMIDT, "Interstitial Compounds" (Butterworth & Co, London, 1967).
3. W. B. PEARSON, "Handbook of Lattice Spacings and Structures of Metals and Alloys" (Vol. I 1958, Vol. II 1969, Pergamon Press, New York).
4. M. HANSEN, "Constitution of Binary Alloys" (McGraw-Hill, New York, 1957; 1st Supplement, R. P. Elliot, 1965; 2nd Supplement, F. A. Shunk, 1969).
5. H. W. KING, in "Alloy Behaviour and Effects in Concentrated Solid Solutions", Ed. T. B. Massalski, AIME Symposium No. 29 (Gordon and Breach Science Publishers, New York, 1965), p. 85.
6. R. SPEISER, J. W. SPRETNAC, and W. J. TAYLOR, *Trans. ASM* **46** (1954) 1168.
7. G. HÄGG, *Z. Physik. Chem. (Leipzig)*, **B.12** (1931) 33.
8. L. S. DARKEN and R. W. GURRY, "Physical Chemistry of Metals" (McGraw-Hill, New York, 1955).
9. J. D. ESHELBY, *Sol. State Phys.* **3** (1956) 79.
10. H. W. KING, in "Physical Metallurgy", Ed. R. W. Cahn (North Holland, Amsterdam, 1965) p. 33.

Received 30 March and accepted 17 May 1971.